Cancer Cell
Article

Microbially Driven TLR5-Dependent Signaling Governs Distal Malignant Progression through Tumor-Promoting Inflammation

Melanie R. Rutkowski,[1] Tom L. Stephen,[1] Nikolaos Svoronos,[1] Michael J. Allegrezza,[1] Amelia J. Tesone,[1] Alfredo Perales-Puchalt,[1] Eva Brencicova,[1] Ximena Escovar-Fadul,[1] Jenny M. Nguyen,[1] Mark G. Cadungog,[2] Rugang Zhang,[3] Mariana Salatino,[4] Julia Tchou,[4,5,6] Gabriel A. Rabinovich,[7] and Jose R. Conejo-Garcia[1,*]
[1]Tumor Microenvironment and Metastasis Program, The Wistar Institute, Philadelphia, PA 19104, USA
[2]Helen F. Graham Cancer Center, Christiana Care Health System, 4701 Ogletown-Stanton Road, Newark, DE 19713, USA
[3]Gene Expression and Regulation Program, The Wistar Institute, Philadelphia, PA 19104, USA
[4]Division of Endocrine and Oncologic Surgery, Department of Surgery
[5]Rena Rowan Breast Center
[6]Abramson Cancer Center, Perelman School of Medicine
University of Pennsylvania, Philadelphia, PA 19104-1693, USA
[7]Laboratorio de Inmunopatología, Instituto de Biología y Medicina Experimental (IBYME-CONICET), Buenos Aires, Argentina
*Correspondence: jrconejo@wistar.org
http://dx.doi.org/10.1016/j.ccell.2014.11.009

SUMMARY

The dominant *TLR5*^{R392X} polymorphism abrogates flagellin responses in >7% of humans. We report that TLR5-dependent commensal bacteria drive malignant progression at extramucosal locations by increasing systemic IL-6, which drives mobilization of myeloid-derived suppressor cells (MDSCs). Mechanistically, expanded granulocytic MDSCs cause γδ lymphocytes in TLR5-responsive tumors to secrete galectin-1, dampening antitumor immunity and accelerating malignant progression. In contrast, IL-17 is consistently upregulated in TLR5-unresponsive tumor-bearing mice but only accelerates malignant progression in IL-6-unresponsive tumors. Importantly, depletion of commensal bacteria abrogates TLR5-dependent differences in tumor growth. Contrasting differences in inflammatory cytokines and malignant evolution are recapitulated in TLR5-responsive/unresponsive ovarian and breast cancer patients. Therefore, inflammation, antitumor immunity, and the clinical outcome of cancer patients are influenced by a common *TLR5* polymorphism.

INTRODUCTION

A rapidly growing paradigm is that commensal microorganisms are required to maintain immune homeostasis of mucosal surfaces such as the intestine (Mazmanian et al., 2008) while facilitating the shaping of immune responses against pathogens in the periphery (Abt et al., 2012; Clarke et al., 2010). Most recently, interactions between microbiota and mucosal surfaces have been demonstrated to have a crucial role in therapeutic responses for tumors occurring outside of the intestinal tract (Iida et al., 2013; Viaud et al., 2013). Although the mechanisms of distal immune regulation by the microbiota are poorly understood, their importance is illustrated by the lack of cellular immune responses and a very narrow T cell repertoire in germ-free mice.

Pattern recognition receptors recognize pathogen-associated molecular patterns, including those contained in commensal

Significance

7.5% of the general population harbor a single dominant nucleotide polymorphism in *TLR5*, resulting in up to an 80% reduction in signaling. We perform a survival analysis of TCGA data sets for individuals with this polymorphism and show that TLR5 signaling affects the malignant progression of ovarian and breast cancer differently. In both TLR5-responsive and nonresponsive mice, depletion of commensal bacteria abrogates differences in tumor progression. We also show that TLR5 recognition of commensal bacteria results in elevated IL-6 levels during tumor progression, whereas, in TLR5 nonresponsive, tumor-bearing mice, there is an increased systemic production of IL-17. Mechanistically, we demonstrate that TLR5 signaling is driving differential tumor-promoting inflammation and that the balance of IL-6 and IL-17 influences the outcome of malignant progression.

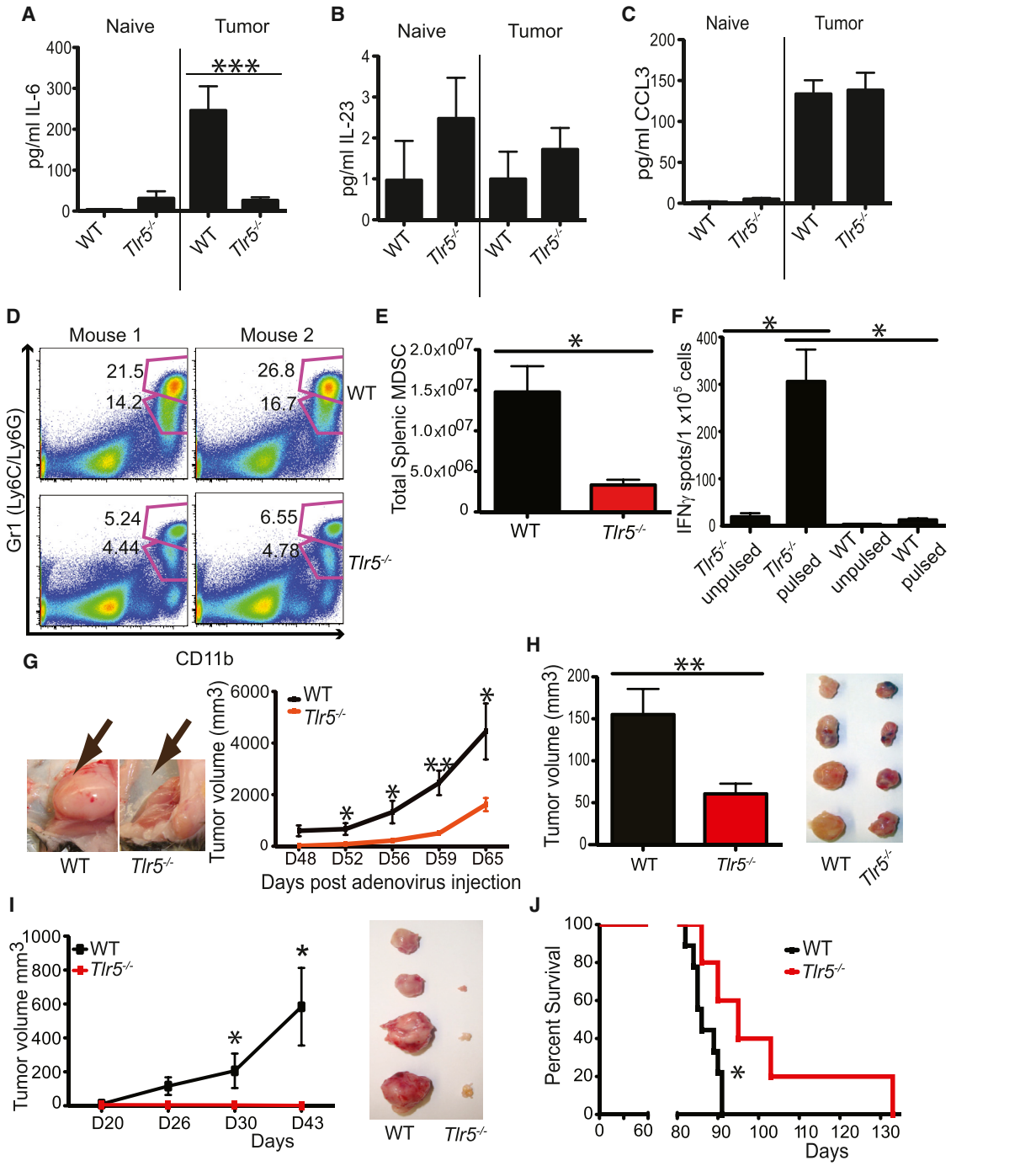

Figure 1. Tumor-Promoting Inflammation Is Driven by TLR5-Dependent Signaling

(A–C) Serum levels of IL-6 (A), IL-23 (B), and CCL3 (C) in TLR5-responsive (WT) and TLR5-deficient (*Tlr5*$^{-/-}$) mice with advanced (days 64–75) flank sarcomas (Tumor, n ≥ 15/group) or naive littermate controls, as detected by ELISA.

(D and E) Proportions (D) and total numbers (E) of MDSC infiltrating into the spleens of WT or *Tlr5*$^{-/-}$ mice bearing equally sized tumors. Shown is one representative of two independent experiments with five to eight animals per group.

(F) IFNγ enzyme-linked Immunospot of sorted antigen-specific CD8 T cells from the draining lymph node (inguinal) of mice bearing day 64 hind flank sarcomas incubated with tumor-lysated, pulsed BMDCs (pulsed) or BMDCs only (unpulsed). Data are representative of two experiments with at least three mice per group.

(G) Representative images of tumors and growth curve of *Tlr5*$^{-/-}$ or WT transgenic mice administered subcutaneous adenovirus-Cre into the hind flank. Data are representative of five individual experiments with at least six to ten mice per group.

(H) Representative final tumor volume and resected ID8-*Vegf-Defb29* tumors 27 days after injection into the axillary flank. Data are representative of two individual experiments with at least five to eight mice per group.

(legend continued on next page)

microbiota. At least 23% of individuals in the general population are carriers of functional polymorphisms in Toll-like receptor (*TLR*) genes (Casanova et al., 2011), but their effect on immunosurveillance against extraintestinal tumors remains poorly understood. One of the most frequent polymorphisms is found in *TLR5*. Approximately 7.5% of the general population harbor a single dominant nucleotide polymorphism in *TLR5* (1174 C > T), encoding a stop codon in place of an arginine at codon 392 ($TLR5^{R392X}$) (Hawn et al., 2003; Misch and Hawn, 2008). This polymorphism results in truncating the transmembrane signaling domain of TLR5 (the specific receptor of flagellin), abrogating signaling by 50%–80%, even for individuals who are heterozygous for this allele. Although the relative frequency of heterozygous carriers within the general population indicates compatibility with a healthy lifestyle, this polymorphism has immunological consequences because heterozygous carriers have an enhanced susceptibility to Legionnaires disease (Hawn et al., 2003), urinary tract infections (Hawn et al., 2009), and bronchopulmonary dysplasia (Sampath et al., 2012). However, virtually nothing is known about the systemic consequences of microbially induced TLR5-dependant signaling, and malignant progression of tumors occurring outside of the intestines.

Here we dissected the role of TLR5 signaling at mucosal surfaces on tumor progression at extramucosal locations through systemic inflammation.

RESULTS

TLR5 Signaling Results in Tumor-Promoting Systemic Inflammatory Responses during Malignant Progression

To determine whether TLR5 signaling influences the malignant progression of extraintestinal tumors, we generated B6 mice with latent mutations in p53 and K-ras ($Trp53^{flx/flx}$;*LSL-*$Kras^{G12D/+}$) (Jackson et al., 2001; Jonkers et al., 2001; Scarlett et al., 2012) on a TLR5-deficient ($Tlr5^{-/-}$) or TLR5-responsive (wild-type [WT]) background. No evidence of metabolic syndrome or colitis in $Tlr5^{-/-}$ mice was observed in our facilities (Figures S1A–S1C available online). Subcutaneous delivery of adenoviruses expressing Cre-recombinase into the hind flank led to concurrent ablation of p53 and activation of oncogenic K-ras, resulting in palpable tumors with histological features of sarcoma. Notably, tumor-bearing (but not naive) WT mice exhibited significantly greater serum levels of IL-6 compared with $Tlr5^{-/-}$ littermates bearing similarly sized tumors (Figure 1A; Figure S1D), whereas other inflammatory cytokines were increased at similar levels or remained unchanged in both groups (Figures 1B and 1C; Figures S1E and S1F).

Consistent with IL-6-mediated systemic inflammation, we found increased mobilization of myeloid-derived suppressor cells (MDSCs) (Figures 1D an 1E)—both $Ly6C^+$ and $Ly6G^+$ (Figure S1G)—in TLR5-responsive mice compared with $Tlr5^{-/-}$ littermates with an equivalent tumor burden. As expected, no TLR5-dependent differences were found in tumor-free mice (Figure S1H). Reconstitution with IL-6-deficient bone marrow (Figure S1I) and antibody-mediated neutralization of IL-6 (Figure S1J) resulted in significant decreases in the mobilization of MDSCs in tumor-bearing WT hosts. Accordingly, tumor-specific effector CD8 T cell responses were significantly impaired in WT animals (Figure 1F) but were restored in tumor-bearing WT animals reconstituted with IL-6-deficient bone marrow (Figure S1K). Correspondingly, tumor growth was increased in TLR5-competent hosts (Figure 1G).

Accelerated malignant progression in TLR5-responsive mice was not driven by TLR5-dependent responses in the tumor cells (e.g., in response to bacterial translocation), as the same tumor cells, or syngeneic p53/K-ras ovarian tumor-derived cells (Scarlett et al., 2012) injected into the axillary flank also progressed significantly faster in TLR5-responsive mice, compared to TLR5-deficient littermates (Figures 1H and 1I). Differences in tumor progression (Figure 1J) and antitumor immunity (Figure S1L) were also recapitulated when ovarian tumor cells were administered intraperitoneally.

No endotoxin could be detected in the serum or tumor ascites (data not shown). More importantly, the background PCR signals for bacterial ribosomal 16S detected in the serum, tumor, draining lymph nodes, or ascites from WT or $Tlr5^{-/-}$ mice were similar to those found in matching control samples from healthy WT mice (Figure S1M).

Taken together, these data indicate that TLR5 signaling is sufficient to drive systemic tumor-promoting inflammation associated with impaired antitumor immunity and accelerated malignant progression and without obvious dysbiosis in TLR5-deficient hosts.

TLR5-Dependent Accelerated Extraintestinal Tumor Growth Is Mediated through Interactions with Commensal Microbiota

Notably, although the composition of the microbiota in TLR5-deficient and TLR5-competent mice was more similar than when compared individually with WT syngeneic mice from a different facility within the campus of the University of Pennsylvania, microbiome-wide differences remained between WT and $Tlr5^{-/-}$ mice after cohousing them in the same cage for 4 weeks (Figures 2A and 2B). Significant differences were found in the genera of *Allobaculum*, *Bacteroides*, and *Lactobacillus*, although not in other species associated with inflammation, such as *Candidatus* Arthromitus or *Clostridia*. In addition, cohoused WT and $Tlr5^{-/-}$ mice retained differences in the progression of both ovarian tumors and transplantable sarcomas generated from p53/K-ras autochthonous tumors (termed MPKAS; Figures 2C–2F). Because mice are naturally coprophagic, differences in the composition of the microbiota after cohousing suggest that the absence of TLR5 activity contributes to forge a dissimilar repertoire of commensal bacteria under similar environmental conditions. To test the influence of TLR5-dependent commensal microorganisms on the progression of extramucosal tumors, we first confirmed significantly elevated serum levels of IL-6

(I) Growth curve and representative resected UPK10 (p53/K-ras-dependent ovarian) tumors 43 days after challenge in the axillary flank. Data are representative of two individual experiments with at least four to six mice per group.
(J) Survival proportions of $Tlr5^{-/-}$ and WT mice bearing syngenic ID8 ovarian tumor cells (≥5/group with two repetitions).
All data represent the mean ± SEM. *$p < 0.05$, ***$p < 0.001$ $Tlr5^{-/-}$ compared with WT using Mann-Whitney test and log rank test for survival. See also Figure S1.

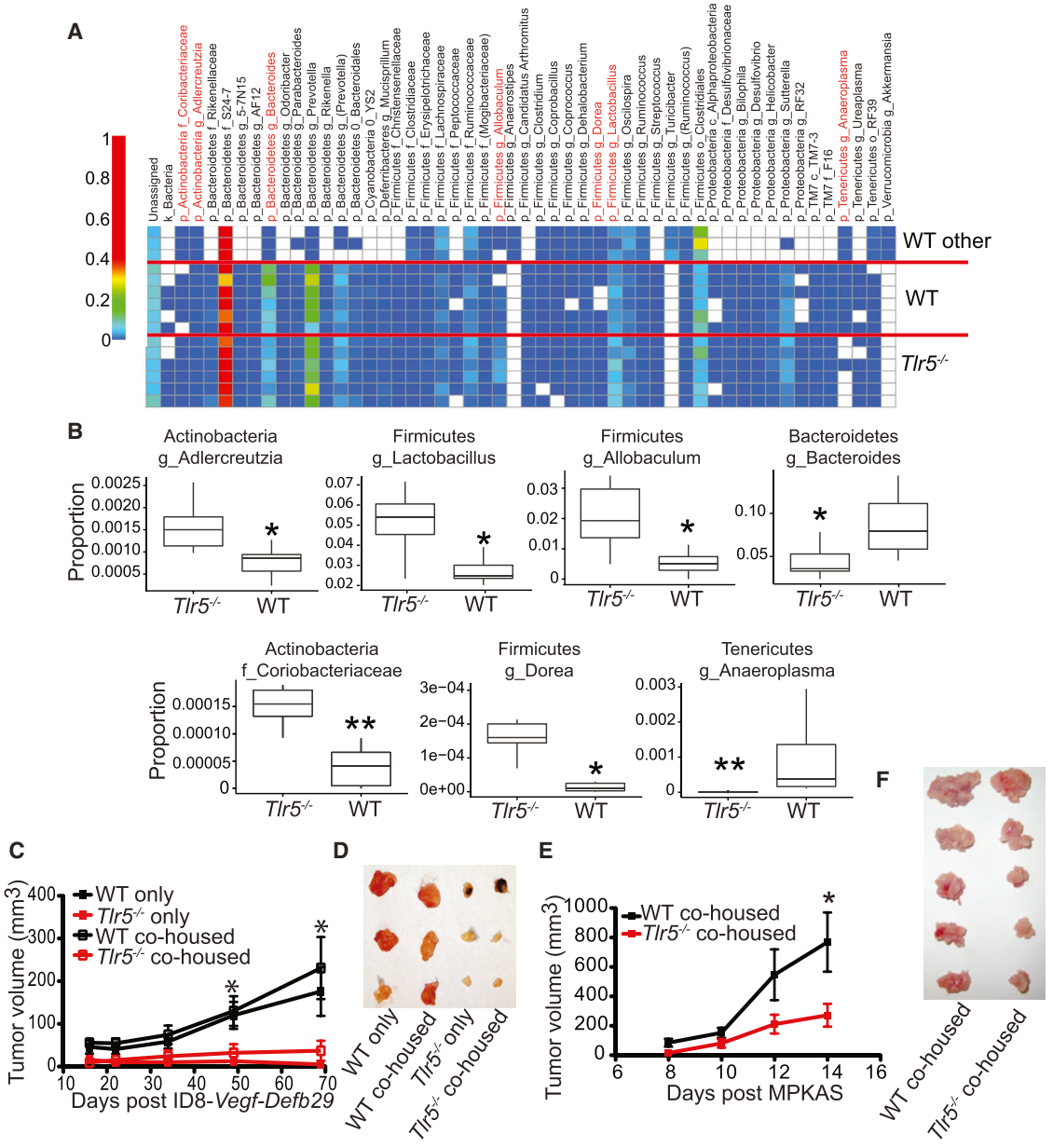

Figure 2. The Absence of TLR5 Signaling Results in a Divergent Microbial Composition and Reduced Tumor Progression

(A) Heatmap of operational taxonomic units of commensal bacterial phyla from WT or *Tlr5*$^{-/-}$ mice cohoused for 4 weeks compared with naive WT mice housed in a different animal facility (WT other).

(B) Proportions of the indicated bacterial phyla in cohoused WT and *Tlr5*$^{-/-}$ mice. Boxes represent the interquartile range (bottom, 25th percentile; top, 75th percentile), and the line inside represents the median. Whiskers denote the lowest and highest values within 1.5× the interquartile range. Kruskal-Wallis one-way ANOVA was used to calculate significance.

(C) Tumor growth kinetics of ID8-*Vegf-Defb29* injected into the axillary flank of WT and *Tlr5*$^{-/-}$ mice cohoused for 4 weeks prior to the injection. Data are representative of one experiment with at least five mice per group.

(D) Tumors from cohoused mice in (C) resected after 69 days.

(E) Growth kinetics of MPKAS sarcomas injected in the axillary flank of WT and *Tlr5*$^{-/-}$ mice cohoused for 3 weeks prior to the injection. Data are representative of one experiment with at least five mice per group.

(F) Resected tumors from cohoused mice in (C) 14 days after injection.

All data represent the mean ± SEM. *p < 0.05, **p < 0.01, ***p < 0.001. Unless stated otherwise, Mann-Whitney test was used.

(Figure 3A) and accelerated tumor growth (Figure 3B) in WT mice challenged with transplantable MPKAS sarcomas. Depletion of commensal microbiota in both TLR5-responsive and deficient mice by oral administration of antibiotics (ABX) resulted in enlarged ceca and a reduction in the burden of bacteria in the intestines, as evidenced by 16 s quantification of the bacterial

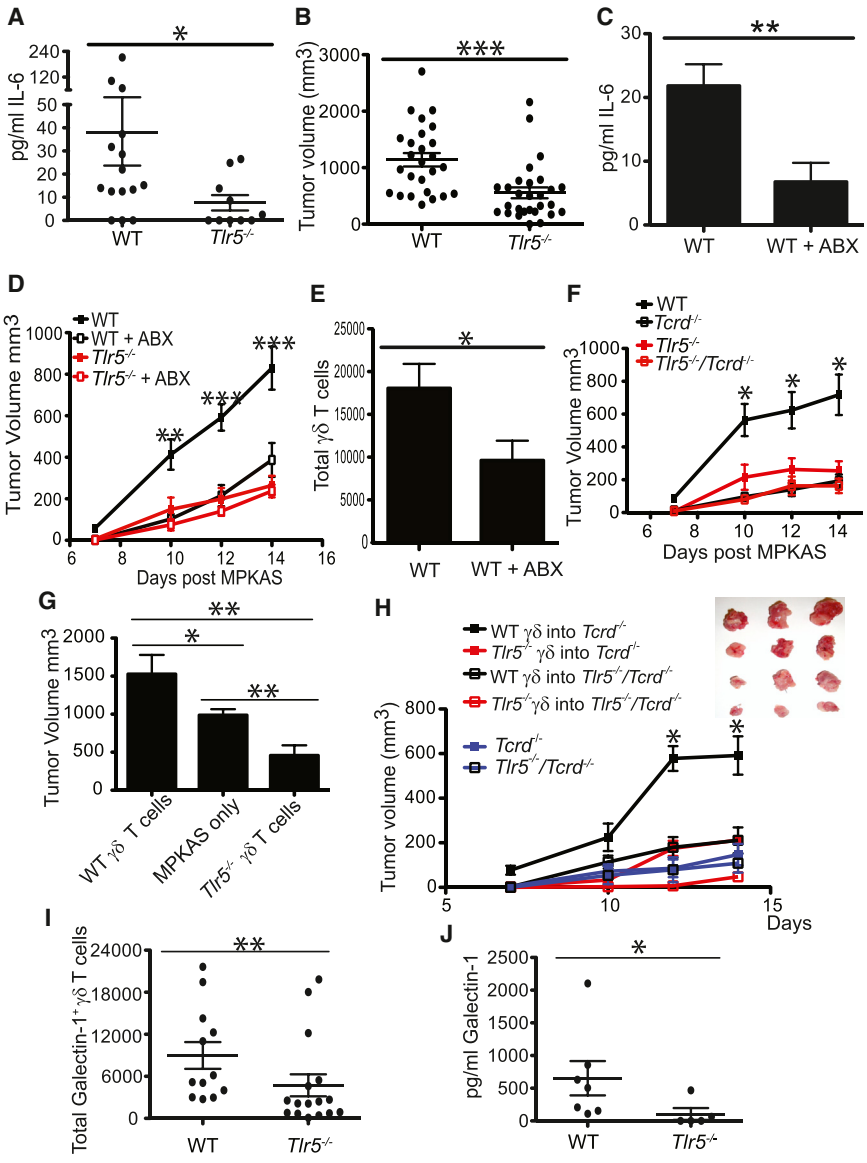

Figure 3. Commensal Microbiota Modulate TLR5-Dependent Tumor Growth through Increased IL-6 and γδ T Cells

(A) IL-6 serum levels of WT or *Tlr5*$^{-/-}$ mice 14 days after being transplanted with the MPKAS sarcoma cell line.

(B) Tumor volume of MPKAS in *Tlr5*$^{-/-}$ or WT mice at day 14 ($n \geq 26$/group).

(C–E) WT and *Tlr5*$^{-/-}$ mice were gavaged daily for 2 weeks with an antibiotic cocktail (ABX) to eliminate the commensal microbiota or with autoclaved H_2O prior to the initiation of MPKAS tumors, and antibiotic depletion was continued throughout the course of tumor progression. IL-6 serum levels in mice 14 days after initiation of MPKAS tumors (C), tumor growth kinetics (D), and total γδ T cells in the draining axillary and brachial lymph node in mice 14 days after initiation of MPKAS tumors (E) are shown. Data are representative of at least three experiments with five mice per group.

(F) Growth kinetics of MPKAS tumors in *Tcrd*$^{-/-}$ or *Tlr5*$^{-/-}$/*Tcrd*$^{-/-}$ mice compared with the appropriate WT and *Tlr5*$^{-/-}$ littermate controls. Data are representative of two individual experiments with at least five to eight mice per group.

(G) Volume of tumors 14 days after transplantation of MPKAS tumor cells alone or together with WT or *Tlr5*$^{-/-}$ tumor-associated γδ T cells into the auxiliary flank of naive WT mice.

(H) Tumor growth curve of MPKAS cells admixed with tumor-associated γδ T cells sorted from WT or *Tlr5*$^{-/-}$ tumor-bearing mice injected into the axillary flank of *Tcrd*$^{-/-}$ or *Tlr5*$^{-/-}$/*Tcrd*$^{-/-}$ mice and representative resected tumors 14 days after the implantation.

(I) Total galectin-1^{+} γδ T cells from tumor-draining lymph nodes of WT or *Tlr5*$^{-/-}$ mice with advanced autochthonous sarcomas.

(J) γδ T cells were sorted from the draining lymph nodes of WT or *Tlr5*$^{-/-}$ mice bearing advanced autochthonous sarcomas and cultured for 6 hr with phorbol 12-myristate 13-acetate/ionomycin. Supernatants were collected and assayed for galectin-1 levels.

All data represent the mean ± SEM. *$p < 0.05$, **$p < 0.01$, ***$p < 0.001$ using Mann-Whitney test. See also Figure S2.

load from fecal pellets of treated and untreated mice (Figures S2A and S2B). Most importantly, differences in systemic IL-6 levels (Figure 3C), mobilization of MDSCs (Figure S2C), and tumor growth (Figure 3D; Figure S2D) were all completely abrogated when commensal bacteria were eliminated from tumor-challenged WT and *Tlr5*$^{-/-}$ mice as a result of significantly delayed tumor progression in WT mice. Correspondingly, bacterial depletion was associated with an increased accumulation of interferon γ (IFNγ)-producing effector CD8 T cells (Figure S2E). Decreased tumor growth could not be attributed to nonspecific antitumor activity of the (oral) antibiotic cocktail because there was no effect on tumor cell proliferation (Figure S2F).

γδ T Cells Promote Tumor Growth through Galectin-1 Secretion in a TLR5-Dependent Manner

Unexpectedly, bacterial depletion resulted in a significant and selective decrease in the number of γδ T cells in the tumor microenvironment (TME) in TLR5-responsive hosts (Figure 3E; Figure S2G). γδ lymphocytes preferentially accumulate at mucosal surfaces, linking innate and adaptive immunity through the secretion of cytokines and chemokines, providing help for adaptive responses, lysing target cells, or directly presenting antigens.

To understand the role of γδ T cells infiltrating into tumors that grow more aggressively in the presence of TLR5 signaling, WT and *Tlr5*$^{-/-}$ littermates deficient of γδ T cells were challenged with syngeneic MPKAS sarcomas. Tumors progressed significantly more slowly in WT mice lacking γδ T cells, whereas tumor growth in *Tlr5*$^{-/-}$ γδ-deficient mice was unchanged (Figure 3F). To verify that tumor-derived γδ T cells were sufficient to accelerate malignant growth only in the presence of TLR5 signaling, γδ T cells were sorted from the draining lymph nodes of WT and *Tlr5*$^{-/-}$ mice with advanced autochthonous p53/K-ras flank sarcomas and admixed with MPKAS tumor cells for injection

into naive WT recipients. Compared with tumor cells administered alone and together with tumor-derived γδ T cells from *Tlr5*$^{-/-}$ mice, γδ T cells from WT mice significantly accelerated tumor growth (Figure 3G). Correspondingly, administration of tumor-associated γδ T cells from TLR5-responsive mice (but not from *Tlr5*$^{-/-}$ mice) enhanced tumor growth in γδ T cell-deficient mice (Figure 3H). However, accelerated malignant progression only occurred in TLR5-responsive hosts, suggesting that intrinsic TLR5-dependent mechanisms regulate the tumor-promoting activity of γδ T cells.

An exhaustive phenotypic analysis of γδ T cells sorted from tumors and draining lymph nodes of WT and *Tlr5*$^{-/-}$ mice did not reveal significant differences in the levels of NKG2D, CD39/CD73, and PD-1 or in the production of IL-10, IFNγ, PGE2, perforin, and IL-2 (Figures S2H–S2K). In contrast, as detectable by intracellular flow cytometry (Figure 3I) and ELISA (Figure 3J), tumor-associated γδ T cells from WT mice produced significantly more immunosuppressive galectin-1. Additionally, antibiotic treatment of mice also resulted in a significant reduction in galectin-1-producing γδ T cells (Figure S2L). Galectin-1 is a pleiotropic molecule that binds to surface glycoconjugates that contain *N*-acetyllactosamine sequences, promoting their crosslinking. Because of the dissimilar glycosylation pattern of different subsets of T helper and effector cells, galectin-1 exerts apoptosis and unresponsiveness on Th1, Th17, and CD8 effector T cells but enhances regulatory T cell activity (Dalotto-Moreno et al., 2013; Rubinstein et al., 2004; Toscano et al., 2007).

Interestingly, exposure of γδ T cells to granulocytic Ly6C^{low}Ly6G^{+} MDSCs sorted from both WT and *Tlr5*$^{-/-}$ tumor-bearing hosts induced a significant upregulation of galectin-1 to a greater extent than monocytic Ly6C^{+}Ly6G^{-} MDSCs sorted from the same hosts or Gr1^{+}CD11b^{+} myeloid cells sorted from the spleens of tumor-free mice, whereas control bone marrow-derived dendritic cells (BMDCs) had negligible effects (Figures 4A–4C). Transwell experiments demonstrated that this was attributable to soluble mediators (Figures 4A and 4B) that were not upregulated by IL-6 or flagellin signaling (Figure S3A). Notably, incubation of naive γδ T cells with different agonists of adenosine, generated at higher levels by granulocytic (compared with monocytic) MDSCs (Ryzhov et al., 2011) increased the proportion of galectin-1^{+} lymphocytes, whereas IL-6, PGE2, or transforming growth factor β alone had no significant effect (Figure S3B). Consequently, depletion of MDSCs in sarcoma-bearing mice resulted in a significant decrease in γδ T cell-derived galectin-1 (Figure 4D), reducing the differences in the growth of tumors between *Tlr5*$^{-/-}$ and WT mice (Figure 4E). Together, these data indicate that MDSCs preferentially mobilized in response to TLR5-dependent, microbiota-driven inflammation and induce γδ T cells in the TME to produce immunosuppressive galectin-1 through soluble factors, including adenosine, causing accelerated tumor growth.

Galectin-1 Secretion Specifically by Immunosuppressive γδ T Cells Is Sufficient to Accelerate Tumor Growth

As expected, tumors grew more slowly in galectin-1-deficient (*Lgals1*$^{-/-}$) mice (Figures S3C and S3D). Other tumor-infiltrating cells, including MDSCs, also produced galectin-1, although at lower levels (Figure S3E). To define whether galectin-1 specifically produced by γδ T cells contributed significantly to differential tumor growth, we generated chimeras with γδ- and galectin-1-deficient mixed bone marrow in p53/K-Ras mice, which were subsequently challenged with adenovirus-Cre to induce tumor formation. As shown in Figure 4F, tumors progressed significantly more slowly when the only γδ T cells in the host were galectin-1-deficient, without defects in the reconstitution of the γδ T cell compartment (Figure S3F). Furthermore, MPKAS tumor cells admixed with galectin-1-deficient γδ T cells from tumor-draining lymph nodes grew significantly slower than MPKAS cells admixed with galectin-1^{+} γδ T cells derived from tumors of identical size or even MPKAS tumors alone (Figures S3G and S3H).

To determine whether galectin-1-producing, tumor-derived γδ T cells inhibit antigen-specific T cell responses, γδ T cells were again sorted from tumor-bearing hosts. As shown in Figure 4G, the antigen-specific proliferation of endogenous tumor-reactive T cells in response to BMDCs pulsed with UV light- and γ-irradiated (immunogenic) tumor cells was impaired significantly in the presence of γδ T cells from syngeneic and autochthonous tumor-bearing, TLR5-responsive mice, whereas γδ T cells from tumor-bearing *Tlr5*$^{-/-}$ hosts did not significantly inhibit proliferation. Most importantly, γδ T cells from WT tumor-bearing hosts impaired the strong proliferation of ovalbumin-specific T cells, whereas their counterparts in galectin-1-deficient mice had no suppressive effect (Figure 4H). Taken together, these data indicate that γδ T cells in TLR5-responsive, but not TLR5-deficient, tumor-bearing hosts are capable of suppressing T cell responses by secreting galectin-1, significantly contributing to malignant progression.

Accelerated Malignant Progression in TLR5-Competent Hosts Depends on Tumor-Derived IL-6

Our results so far indicated that TLR5 signaling at places of bacterial colonization in tumor-bearing hosts induced tumor-promoting systemic inflammation, resulting in the mobilization of MDSCs and immunosuppressive γδ T cells. To define the general applicability of these findings, WT and *Tlr5*$^{-/-}$ mice were challenged with multiple tumor models, and the growth was compared. TC-1 cells and ovarian cancer cell lines generated from a p53/K-ras model (Scarlett et al., 2012) grew significantly faster in TLR5-competent syngeneic mice (Figure 1I and data not shown). Unexpectedly, syngeneic A7C11 mammary tumor cells, derived from autochthonous p53/K-ras-dependent mammary carcinomas (Rutkowski et al., 2014), progressed faster in TLR5-deficient mice in multiple independent experiments (Figure 5A). Serum levels of IL-6 in this system were much lower than in tumors that progressed more rapidly in WT mice and were independent of tumor burden or TLR5 signaling (Figure 5B). Comparable results were obtained with different clones derived from autochthonous mammary tumors concurrently carrying myristoylated (constitutively activated) p110α (termed BRPKP110 cells; Figure S4A). Notably, exogenous IL-6 had negligible effects on the upregulation of IL-6 in A7C11 cells (Figure 5C), although STAT3 was effectively activated (Figure S4B), and tumor cells expressed the IL-17 receptor, IL-6, receptor and gp300 (Figures S4C and S4D). In contrast, tumors that induced TLR5-dependent systemic IL-6 upregulation

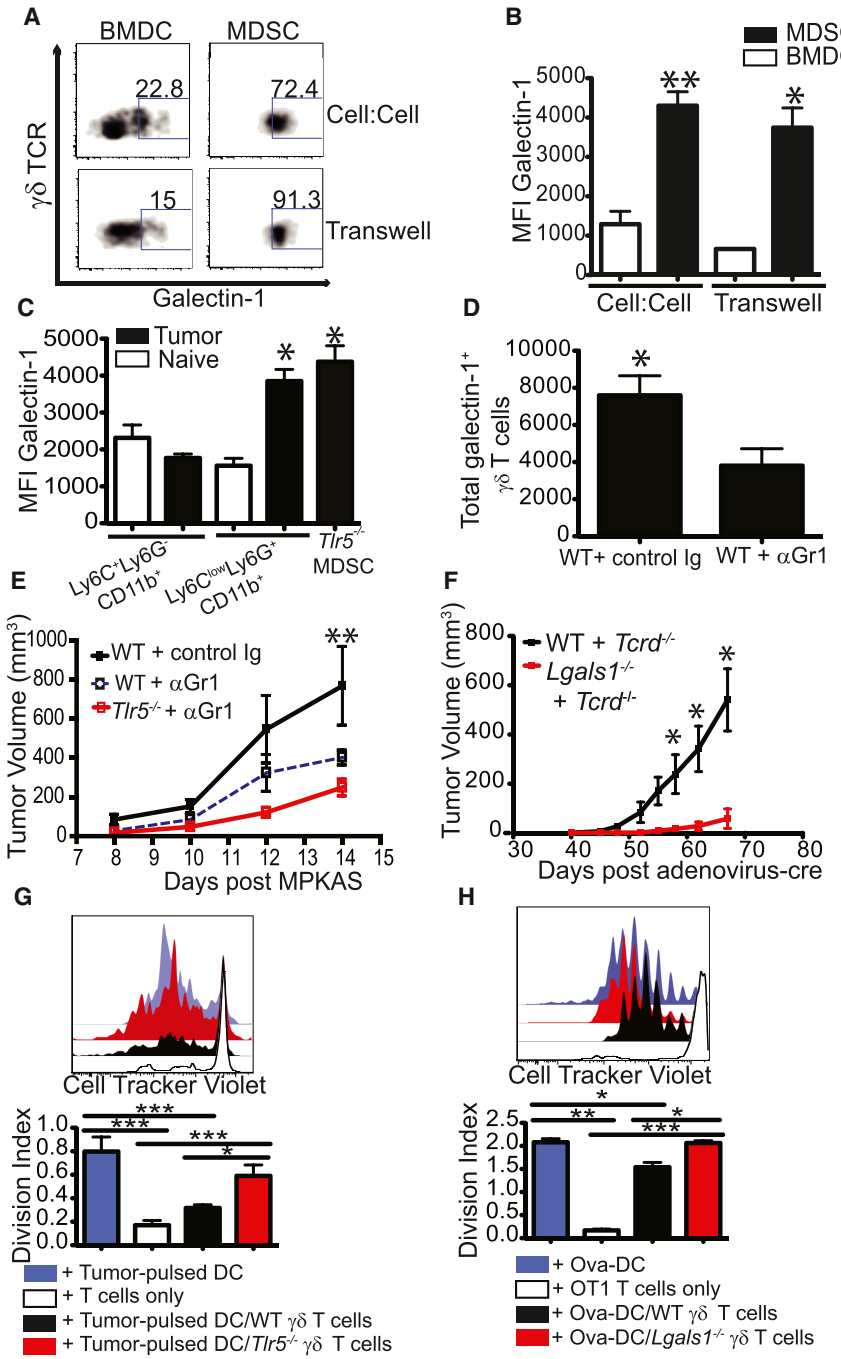

Figure 4. Galectin-1-Producing γδ T Cells Are Sufficient to Promote Accelerated TLR5-Mediated Malignant Progression

(A and B) Scatter plots (A) and median fluorescence intensity (MFI) (B) of intracellular galectin-1 expression of naive γδ T cells sorted from pooled axillary and inguinal lymph nodes of WT mice and incubated directly (Cell:Cell) or separated by a transwell insert (Transwell) for 5 days with MDSCs sorted from the spleens of WT mice carrying advanced autochthonous sarcomas or with bone marrow-derived dendritic cells from naive WT mice (BMDC).

(C) MFI of intracellular galectin-1 expression from naive γδ T cells cocultured with monocytic ($Ly6C^+Ly6G^-$) and granulocytic ($Ly6C^{low}Ly6G^+$) MDSCs from tumor-bearing WT mice or with total MDSCs from tumor-bearing *Tlr5*$^{-/-}$ mice. Polymorphonuclear leukocytes and monocytes were sorted from the spleens of naive WT mice as controls.

(D) Total galectin-1$^+$ γδ T cells in the draining lymph nodes of WT MPKAS tumor-bearing mice depleted of MDSCs (αGr1). Ig, immunoglobulin.

(E) Representative MPKAS tumor growth curve in WT mice depleted of MDSCs.

(F) Representative tumor growth curve after reconstitution of *Trp53*$^{flx/flx}$;*LSL-Kras*$^{G12D/+}$ mice with bone marrow from WT or *Lgals1*$^{-/-}$ mice admixed (1:1) with *Tcrd*$^{-/-}$ bone marrow, followed by tumor initiation with adenovirus-Cre.

(G and H) γδ T cells sorted from the draining lymph nodes of WT or *Tlr5*$^{-/-}$ mice bearing advanced autochthonous sarcomas or D14 MPKAS tumors and incubated at a 10:10:1 ratio with CellTracker Violet-labeled endogenous tumor-reactive T cells sorted from advanced sarcoma-bearing mice incubated with MPKAS-pulsed dendritic cells (G) or OT-1 T cells and BMDCs pulsed with full-length ovalbumin (Ova) (H). Proliferation of tumor-reactive T cells was measured by flow cytometric analysis five days later.

Data are representative of two independent experiments (five mice total). All data represent the mean ± SEM. *p < 0.05, **p < 0.01, ***p < 0.001 (Mann-Whitney test). See also Figure S3.

responded to exogenous IL-6 by producing high levels of the same cytokine (Figure 5C).

Confirming the contribution of TLR5-dependent, tumor-derived IL-6 to accelerated malignant growth, silencing IL-6 secretion in MPKAS tumor cells with two different constructs resulted in significantly reduced growth of tumors in vivo, whereas no differences were observed in vitro (Figure 5D; Figures S4E–S4G). Notably, mice growing IL-6-silenced sarcomas induced significantly reduced serum IL-6 levels compared with scrambled small hairpin RNA (shRNA)-expressing controls (Figure 5E). Decreased systemic IL-6 resulted in a significant reduction in the accumulation of MDSCs and, correspondingly, diminished production of galectin-1 by γδ T cells (Figures 5F and 5G) and decreased tumor-associated MDSCs (Figure S4H). As a result, a significant increase in the accumulation of IFNγ-producing CD8 T cells was observed in these tumors (Figure 5H; Figure S4I). Leukocyte-derived IL-6 also contributed to the systemic overexpression of IL-6 because reconstitution of mice with IL-6-deficient bone marrow resulted in a dramatic decrease in tumor growth (Figure 5I) and was associated with decreased galectin-1$^+$ γδ T cells (Figure S4J). Correspondingly, accelerated malignant progression in TLR5-responsive hosts was completely abrogated upon IL-6 neutralization (Figure 5J). Together, these results demonstrate that

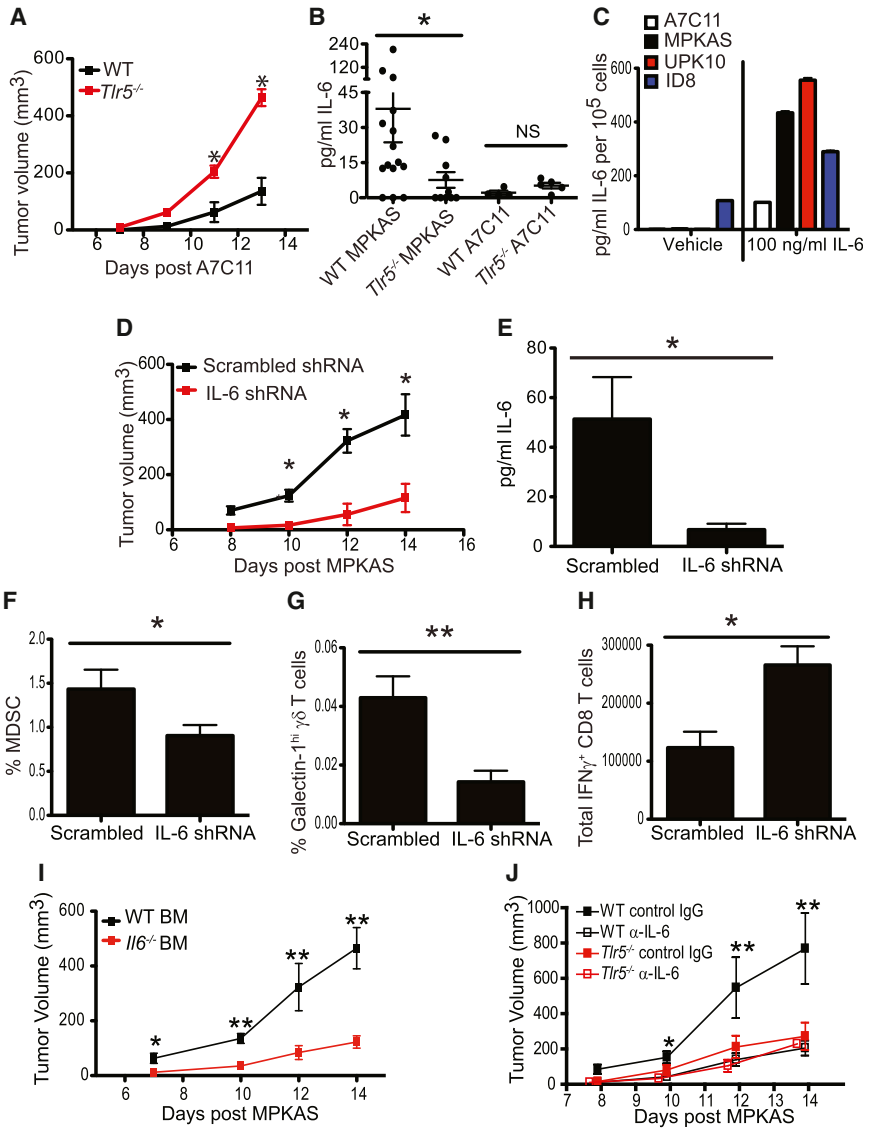

Figure 5. Tumor- and Leukocyte-Derived IL-6 Drives Tumor Growth in TLR5-Responsive Mice

(A) Growth kinetics of the mammary tumor cell line A7C11 in WT or *Tlr5*$^{-/-}$ mice.

(B) Serum IL-6 level of WT or *Tlr5*$^{-/-}$ mice bearing advanced A7C11 (days 14–16) tumors.

(C) ELISA quantification of IL-6 production by the indicated tumor cell lines 72 hr after overnight incubation with 100 ng/ml recombinant mouse IL-6 followed by washing of wells and the addition of fresh media.

(D) Growth kinetics of MPKAS expressing IL-6 shRNA or scrambled shRNA in WT mice.

(E) Serum levels of IL-6 in WT mice 14 days after injection with MPKAS expressing IL-6 shRNA or scrambled control. Shown is one representative of two independent experiments (eight mice per group total).

(F–H) Proportions of tumor-associated Gr1^{+} CD11b^{+} MDSCs (F), galectin-1-producing γδ T cells (G), and IFNγ-producing CD8 T cells (H) from dissociated tumors (F) and tumor-draining lymph-nodes (G and H) 14 days after injection of WT mice with MPKAS tumor cell lines expressing IL-6 shRNA or scrambled shRNA.

(I) Tumor kinetics of WT mice reconstituted with IL-6-deficient (*Il6*$^{-/-}$) or WT bone marrow (BM) followed by challenge with the MPKAS tumor cell line.

(J) Tumor kinetics of WT or *Tlr5*$^{-/-}$ mice administered IL-6 neutralizing antibody (α-IL-6) or isotype control IgG challenged with MPKAS tumors.

All data represent the mean ± SEM. *p < 0.05, **p < 0.01, ***p < 0.001, NS, not significant (Mann Whitney test). See also Figure S4.

both tumor- and leukocyte-derived IL-6 contribute to accelerate the progression of IL-6-responsive tumors in TLR5-sufficient hosts.

IL-17 Secreted through Interactions with Commensal Bacteria Accelerates Malignant Progression Only in IL-6-Unresponsive Tumors

These results suggest that only IL-6-responsive tumors undergo TLR5-dependent accelerated growth, whereas IL-6-unresponsive tumors rely on other signals. Supporting this proposition, TLR5-deficient mice with advanced A7C11 tumors had significantly higher serum levels of IL-17 compared with WT tumor-bearing mice (Figure 6A). Increased systemic IL-17 was also observed in TLR5-deficient mice growing orthotopic ovarian cancer (Figure S5A) and MPKAS and autochthonous p53/K-ras-dependent flank tumors (Figures 6B and 6C). Despite increased systemic levels of IL-17 in *Tlr5*$^{-/-}$ tumor-bearing mice, we found only minor differences in the ratio of tumor-infiltrating IL-17^{+} cells, which included CD4 and γδ T cells in similar proportions (Figures S5B and S5C).

To define the contribution of IL-17 to accelerated tumor progression in TLR5-deficient hosts, we neutralized IL-17 in A7C11 tumor-challenged *Tlr5*$^{-/-}$ and WT littermates. Blockade of IL-17 abrogated differences in the progression of these tumors in WT versus *Tlr5*$^{-/-}$ hosts, resulting in a significant reduction of tumor burden and growth kinetics in *Tlr5*$^{-/-}$ mice (Figure 6D; Figure S5D).

In contrast, IL-17 neutralization had no effect in the progression of IL-6-dependent MPKAS tumors (Figure 6E; Figure S5E). Remarkably, silencing IL-6 production in the same tumor cells was sufficient to render sarcomas sensitive to the tumor-promoting activity of IL-17 because IL-17 blockade reduced malignant progression in otherwise identical tumors transduced with IL-6-shRNA (Figure 6F). Consistent with the elevation of systemic IL-17 in all *Tlr5*$^{-/-}$ tumor-bearing mice, IL-6 silencing in MPKAS sarcomas was sufficient to reverse the effects of TLR5 signaling on malignant evolution because the same tumors that previously grew faster in WT hosts started progressing more rapidly in *Tlr5*$^{-/-}$ mice when IL-6 was silenced (Figure 6G). Therefore, although IL-6 is systemically upregulated in IL-6-responsive tumors through TLR5 signaling and typically

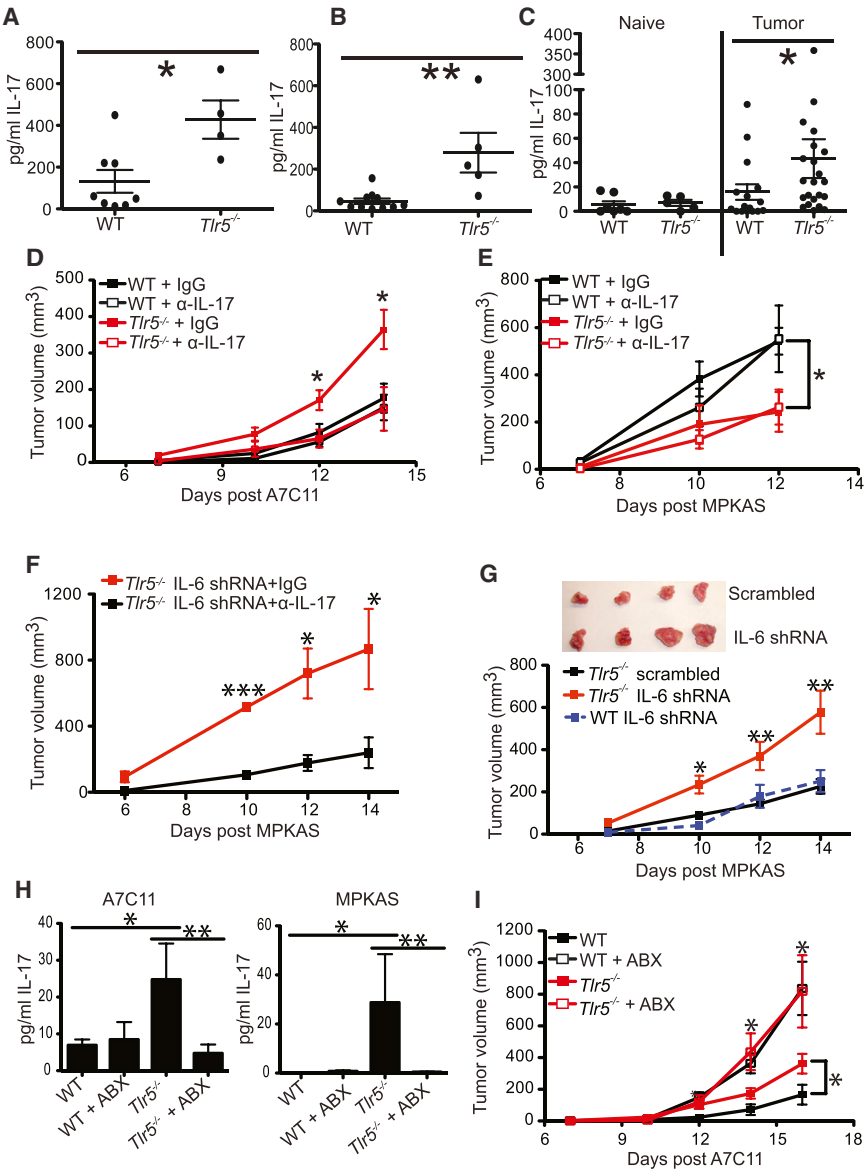

Figure 6. Tumor Growth for IL-6-Unresponsive Tumors Is Mediated by IL-17 Induced by Interactions with Commensal Microbiota

(A–C) Serum levels of IL-17 from WT or *Tlr5*$^{-/-}$ mice bearing advanced A7C11 mammary tumors (A), advanced MPKAS tumors (B), or advanced autochthonous sarcomas from naive controls (C).

(D) A7C11 growth kinetics in WT and *Tlr5*$^{-/-}$ mice administered IL-17 neutralizing antibody (α-IL-17) or Ig control (IgG).

(E) MPKAS tumor kinetics in WT or *Tlr5*$^{-/-}$ mice treated with α-IL-17 or IgG.

(F) Growth kinetics of MPKAS tumors expressing IL-6 shRNA or scrambled shRNA in *Tlr5*$^{-/-}$ mice administered α-IL-17 or IgG.

(G) Growth kinetics of MPKAS expressing IL-6 shRNA or scrambled shRNA in *Tlr5*$^{-/-}$ and WT mice and representative resected tumors from *Tlr5*$^{-/-}$ mice.

(H) Serum levels of IL-17 in ABX or vehicle-treated MPKAS or A7C11 tumor-bearing mice 14 days (MPKAS) or 16 days (A7C11) after tumor initiation.

(I) Growth kinetics of A7C11 tumors from WT and *Tlr5*$^{-/-}$ mice treated with ABX or vehicle.

All data are representative of at least two repetitions with at least four animals per group. All data represent the mean ± SEM. *p < 0.05, **p < 0.01, ***p < 0.001 using Mann-Whitney test. See also Figure S5.

dominates tumor-promoting inflammation in TLR5-competent hosts, IL-17 accelerates malignant progression in IL-6-unresponsive tumors. Because IL-17 is systemically higher in TLR5-deficient, tumor-bearing hosts, the progression of tumors associated with relatively low levels of IL-6 is accelerated.

Notably, antibiotic depletion of commensal bacteria also induced a significant decrease in serum IL-17 levels and, correspondingly, reduced IL-17 producing cells in the draining lymph nodes of *Tlr5*$^{-/-}$ tumor-bearing mice (Figure 6H; Figure S5F), resulting in the complete abrogation of differences in tumor progression between *Tlr5*$^{-/-}$ and WT littermates (Figure 6I; Figure S5G). Together, these results indicate that the balance of IL-6 and IL-17 influence the outcome of malignant progression. Because IL-17 is overproduced in TLR5-deficient, tumor-bearing individuals, in the absence of IL-6, this cytokine predominately drives tumor-promoting inflammation. These results demonstrate that both IL-6- and IL-17-driven inflammatory macro- and microenvironments are controlled by the commensal microbiota and influence malignant progression.

TLR5-Deficient Breast Cancer Patients Show Accelerated Malignant Progression and Upregulation of IL-17 in the TME

To substantiate the relevance of our mechanistic observations, we first confirmed that CD45^{+}CD14^{+} myeloid leukocytes sorted from freshly dissociated human ovarian tumors of three *TLR5*^{R392X} heterozygous carriers showed negligible induction of IL-8 transcript levels in response to flagellin compared with the same cell population sorted from three patients homozygous for the ancestral allele (Figure 7A). These results corroborate previous reports demonstrating that *TLR5*^{R392X} carriers are functionally unable to respond to bacterial flagellin (Gewirtz et al., 2006; Hawn et al., 2003). Most importantly, a survival analysis performed from fully or partially sequenced samples of estrogen receptor-positive (ER^{+}) breast cancer patients from The Cancer Genome Atlas (TCGA) data sets identified a significantly poorer outcome for carriers of the *TLR5*^{R392X} allele compared with patients homozygous for the ancestral *TLR5* allele (Figure 7B).

Supporting the relevance of our observations in murine tumor models, IL-17A transcript levels in our ER^{+} breast cancer and ovarian carcinoma specimens were also significantly higher in *TLR5*^{R392X} carriers compared with control patients homozygous for the ancestral allele (Figure 7C). Both γδ and αβ (CD3^{+}γδ TCR^{-})

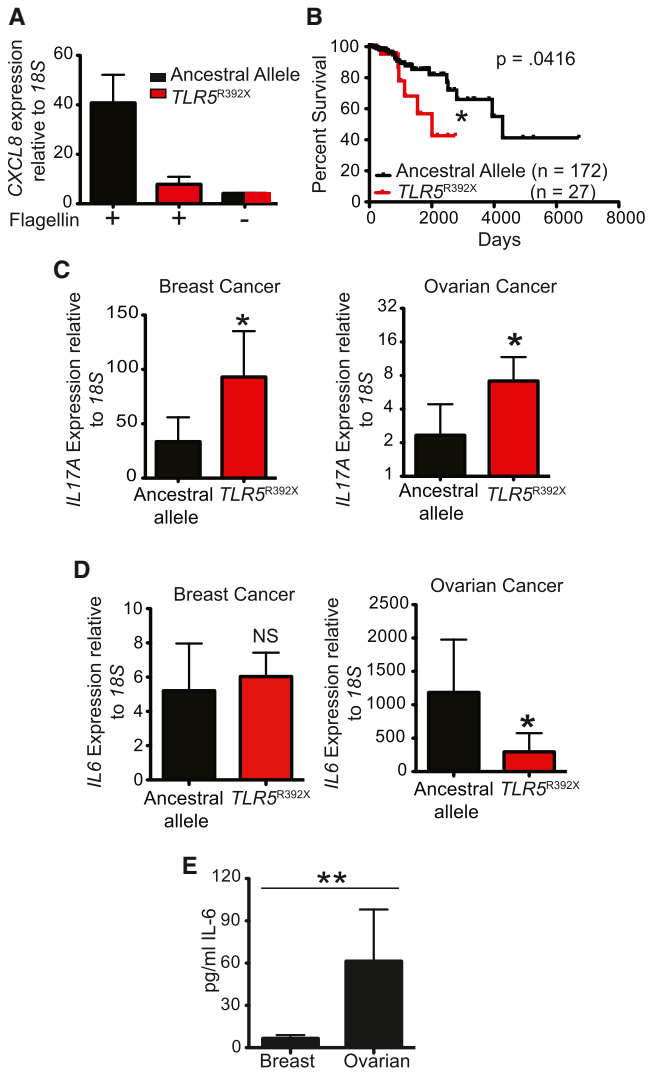

Figure 7. TLR5-Deficient Patients Diagnosed with Breast Cancer Have Accelerated Malignant Progression and Increased Intratumoral IL-17 Levels

(A) *CXCL8* transcript levels in $CD14^+CD45^+$ myeloid cells sorted from three heterozygous $TLR5^{R392X}$ or three TLR5-responsive advanced ovarian tumors and incubated with 500 ng/ml of flagellin for 72 hr. *CXCL8* transcript levels were calculated relative to *18S* expression.

(B) Survival analysis of TCGA data sets for ER^+ breast cancer. Differences in overall survival were calculated with log rank.

(C and D) Quantification of *IL17A* (C) or *IL6* (D) transcripts relative to *18S* expression in nine frozen ER^+ breast tumor specimens from $TLR5^{R392X}$ carriers, ≥10 randomly selected ER^+ breast tumors from patients homozygous for the ancestral allele, five to six stage III/IV ovarian carcinoma specimens from $TLR5^{R392X}$ carriers, and ≥ 15 randomly selected ovarian carcinoma specimens homozygous for the ancestral allele.

(E) Serum IL-6 levels in patients homozygous for the ancestral allele of *TLR5* diagnosed with ER^+ breast carcinoma versus ovarian carcinoma.

All data represent the mean ± SEM. *p < 0.05, **p < 0.01, ***p < 0.001 (Mann-Whitney test). See also Figure S6.

T cells contributed to IL-17 production in breast and ovarian tumors (Figures S6A and S6B). However, significant differences in IL-6 transcript levels were only observed between TLR5-responsive and nonresponsive ovarian tumor specimens but not between TLR5-responsive and nonresponsive ER^+ breast tumor specimens (Figure 7D), further supporting the contribution of tumor-derived IL-6 to differences in overall tumor-promoting inflammation. Additionally, we found much lower levels of circulating IL-6 in 20 available serum samples from ER^+ breast cancer patients compared with sera from 12 available ovarian cancer patients (all of them TLR5-responsive; Figure 7E). These data further support the fact that, in hosts where TLR5-dependent IL-6 does not dominate systemic tumor-promoting inflammatory responses through dramatic systemic upregulation, tumors grow faster in the presence of IL-17 overexpression, which is higher in the absence of TLR5 signaling. Together, these studies demonstrate that a common genetic polymorphism, present in >7% of individuals in the general population (Hawn et al., 2003), influences systemic inflammatory responses and determines the outcome of breast cancer patients.

Higher Proportions of Long-Term Survivors among TLR5-Defective Ovarian Cancer Patients

To further investigate the link between IL-6 upregulation and accelerated tumor progression in the presence of TLR5 signaling, we next analyzed ovarian cancer TCGA data sets. A total number of 25 $TLR5^{R392X}$ patients with outcome and deep sequencing information was insufficient to identify significant differences in overall survival compared with homozygous carriers of the ancestral allele. However, the proportion of long-term survivors (≥6 years after the ovarian cancer diagnosis) was significantly higher among $TLR5^{R392X}$ carriers (but not carriers of other nonfunctional polymorphisms; Figures 8A and 8B), indicating that, as in our orthotopic ovarian preclinical model, TLR5 signaling drives accelerated malignant progression in ovarian cancer.

As in our murine models, the expression of immunosuppressive galectin-1 was significantly higher in TLR5-responsive ovarian cancer patients from our tumor bank, at both transcript and protein levels (Figures 8C and 8D). Furthermore, we found that, in multiple samples, $CD3^+CD4^-CD8^-$ γδ T cells outnumbered $Foxp3^+$ regulatory T cells in the ovarian cancer microenvironment, representing up to ~6% of tumor-infiltrating lymphocytes, as detected by histology (Figure 8E and data not shown) and flow cytometry (Figure 8F). At least 20% of ovarian cancer-infiltrating γδ T cells, which predominantly represent peripheral blood-derived $V\gamma9^+$ lymphocytes, produced significant levels of galectin-1 (Figure 8F). Further supporting the relevance of our observations on the mechanistic role of γδ T cells in the TME, tumors from patients carrying $TLR5^{R392X}$ contained a significantly lower number of galectin-1-producing γδ T cells (Figure 8G) compared with patients homozygous for the ancestral allele. In addition, γδ T cells in tumors from TLR5-responsive patients had significantly higher levels of intracellular galectin-1 on a per-cell basis (Figure 8H) and at significantly higher levels than in tumor-associated MDSCs (Figures S7A and S7B). Nevertheless, higher proportions of galectin-1^+ myeloid leukocytes were also found in dissociated tumors from patients with the ancestral TLR5 allele (Figure S7C). Therefore, supporting the relevance of our preclinical models, these findings reveal that a frequent polymorphism abrogating TLR5 responses to flagellin profoundly

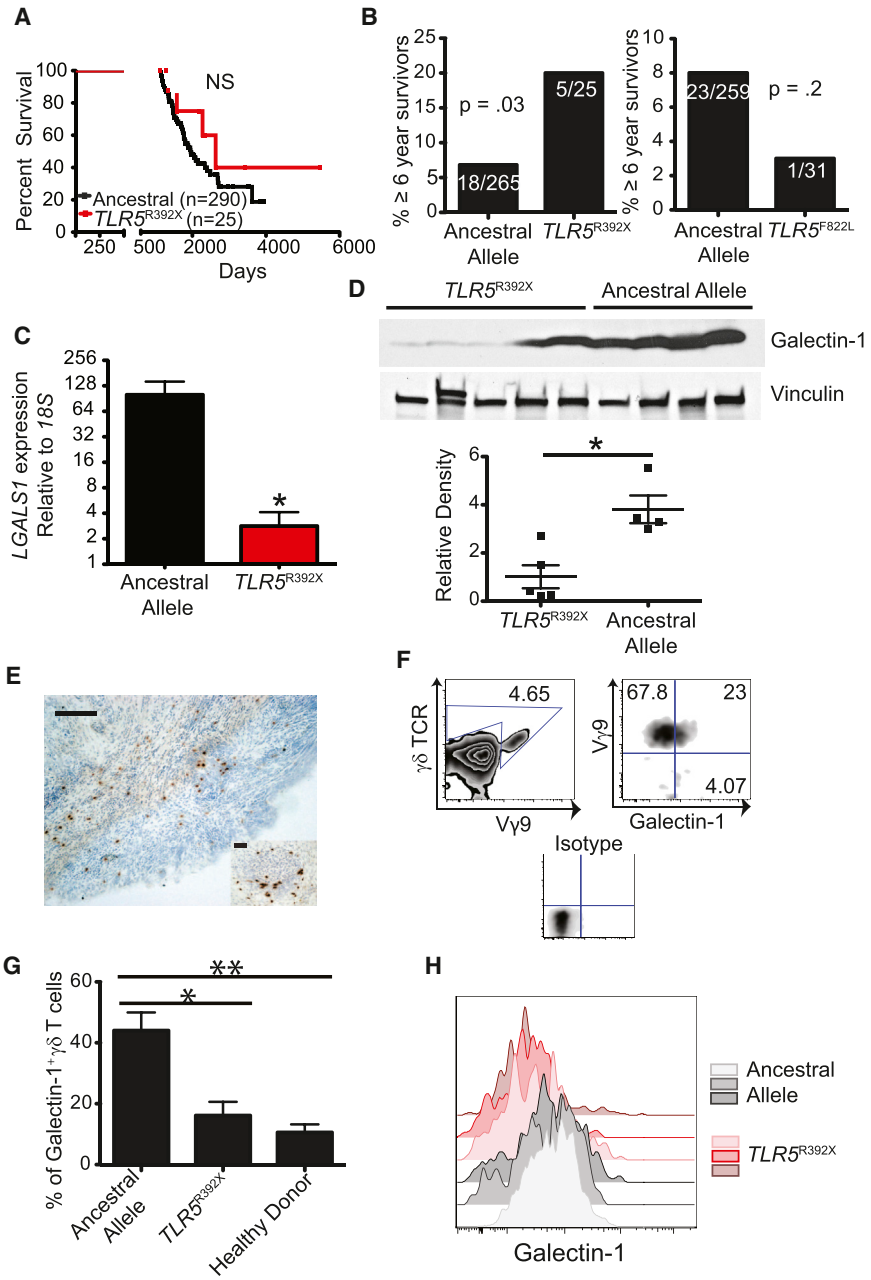

Figure 8. Higher Proportions of Long-Term Survivors and Decreased Galectin-1 Expression Are Found in TLR5-Deficient Patients Diagnosed with Ovarian Cancer

(A) Survival analysis of TCGA data sets for ovarian cancer. The difference was calculated with log rank.

(B) Fisher's exact test of the proportions of ovarian cancer patients surviving longer than or equal to 6 years after initial diagnosis with or without the *TLR5*^{R392X} polymorphism or with or without the nondeleterious *TLR5*^{F822L} polymorphism.

(C) Transcript levels of *LGALS1* relative to *18S* levels from six ovarian tumor samples with *TLR5*^{R392X} and 91 randomly selected ovarian tumor samples homozygous for the ancestral allele of *TLR5*.

(D) Galectin-1 protein expression of 5 *TLR5*^{R392X} ovarian tumor samples and four randomly selected ovarian tumor samples from patients homozygous for the ancestral allele of *TLR5*. Shown is a corresponding densitometric analysis of band intensities for galectin-1 normalized to vinculin.

(E) γδ T cell immunohistochemistry from a frozen ovarian tumor specimen homozygous for the *TLR5* ancestral allele. *Scale bars*, 100 μm.

(F) Representative gating strategy for flow cytometric analysis of galectin-1-expressing, tumor-infiltrating γδ T cells. Numbers represent the proportions of live cells gated from CD45$^+$CD3$^+$γδ TCR$^+$ tumor-associated microenvironmental leukocytes compared with the isotype control.

(G) Frequency of galectin-1-producing γδ T cells in the ovarian cancer microenvironment from three ovarian tumors from *TLR5*^{R392X} carriers, PBMCs from four healthy donors, and 12 randomly selected ovarian tumor samples from patients homozygous for the ancestral allele.

(H) Histogram of galectin-1 expression from tumor-associated γδ T cells from the three available disassociated ovarian tumor samples from *TLR5*^{R392X} carriers and three randomly selected ovarian tumor samples from patients homozygous for the ancestral allele of *TLR5*.

All data represent the mean ± SEM. *$p < 0.05$, **$p < 0.01$, ***$p < 0.001$ (Mann-Whitney test). See also Figure S7.

influences the inflammation orchestrated by extraintestinal tumors and, subsequently, their clinical progression.

DISCUSSION

Our study demonstrates that TLR5 recognition of commensal microbiota regulates systemic tumor-promoting inflammation and, subsequently, extramucosal malignant progression. In some tumors, TLR5 signaling drives the systemic upregulation of IL-6, promoting MDSC mobilization, induction of suppressive galectin-1-producing γδ T cells and, subsequently, accelerated tumor growth. Accordingly, most tumors tested progressed significantly more slowly in TLR5-deficient individuals. In contrast, IL-17 is commonly upregulated in TLR5-deficient, tumor-bearing hosts but only drives accelerated tumor growth in systems where tumor cells are poorly responsive to IL-6. Any differences in malignant evolution are completely abrogated following depletion of commensal bacteria.

Interestingly, TLR5-dependent increased systemic IL-6 is triggered during tumor initiation because it does not occur in tumor-free hosts. TLR5-dependent tumor growth appears to require IL-6 production by both hematopoietic and tumor cells because only IL-6-responsive tumor models are able to induce IL-6-driven MDSC mobilization and subsequent accelerated tumor progression compared with TLR5-nonresponsive animals. Accordingly, knockdown of IL-6 in IL-6-responsive tumor cell

lines significantly diminishes in vivo tumor growth in TLR5-responsive mice, which is associated with decreased serum IL-6 and, subsequently, reduced mobilization of MDSCs and diminished production of galectin-1 by γδ T cells. Supporting the crucial role of IL-6 in tumor-promoting inflammation, in luminal (although not in triple-negative) breast tumors, where systemic IL-6 is significantly lower (e.g., compared with ovarian cancer patients) (Casanova et al., 2011), tumors grow faster in TLR5-defective individuals because IL-17 overexpressed in the TME drives tumor-promoting inflammation. The role of IL-17 during tumor progression remains controversial because it has a clear protective role during ovarian cancer progression but is associated with malignant promotion in other tumors, such as breast cancer (Kryczek et al., 2009; Wang et al., 2009). In our preclinical models, IL-17 neutralization delayed tumor growth only when IL-6 was systemically low but had no effect on tumors that progress faster in TLR5-responsive individuals in an IL-6-dependent manner. Of note, silencing IL-6 was sufficient to transform IL-6-dependent, IL-17-insensitive tumors that grow faster in TLR5-responsive hosts into tumors that become sensitive to IL-17 neutralization and progress faster in TLR5-deficient individuals. The effects of other inflammatory cytokines, therefore, add another layer of complexity to the role of IL-17 in cancer and provide an understanding for its conflicting activities. Most importantly, all differences in tumor-promoting inflammation and malignant progression are eliminated upon depletion of the microbiota. We identified TLR5-dependent microbiome-wide differences in the repertoire of commensal bacteria that persisted after cohousing mice in the same cage. The composition of the microbiota is therefore different in the absence of TLR5 signaling, and this influences tumor-promoting inflammation.

Our results also underscore the contribution of γδ T cells to immunosuppression in multiple tumors, including ovarian cancer. Although the regulatory activity of γδ T cells in breast cancer has been reported (Peng et al., 2007), the mediators of effector T cell suppression remained elusive. We demonstrate that bulk populations of galectin-1-secreting γδ T cells suppress T cell responses to potent antigens in vitro and that galectin-1 specifically produced by tumor-derived γδ T cells is sufficient to accelerate tumor growth in vivo. Galectin-1 has emerged as a crucial driver of immunosuppression in multiple tumors (Rabinovich and Croci, 2012). Secreted galectin-1 crosslinks cell surface glycoconjugates bearing multiple units of the *N*-acetyllactosamine (Galβ1-4-NAcGlc) disaccharide and selectively blunts Th1, Th17, and CD8 effector T cell responses (Rubinstein et al., 2004). Our study identifies γδ T cells as a relevant source of this tolerogenic factor in the TME.

Finally, the most significant conclusion of our study is that frequent polymorphisms that abrogate TLR5 activity are associated with the outcomes of cancer patients. TLR5-dependent differences in survival are particularly striking for ER^+ patients, for whom a TLR5 deficiency is associated with accelerated malignant progression. In contrast, in ovarian cancer patients who have higher serum IL-6, TLR5 signaling has a negative effect on the proportion of long-term survivors. Because at least 30% of individuals in the general population are carriers of a limited set of polymorphisms in multiple pattern recognition receptor genes that could also influence tumor-promoting inflammation (Casanova et al., 2011; Hugot et al., 2007), our study opens avenues for understanding how differential inflammatory responses and, subsequently, dissimilar malignant progression takes place in many cancer patients. Our work also provides a rationale for manipulating the microbiota through antibiotic treatment to modulate tumor-promoting inflammation.

EXPERIMENTAL PROCEDURES

Mice

Transgenic *Kras*^{tm4Tyj} and *Trp53*^{tm1Brn} mice (Jackson et al., 2001; Jonkers et al., 2001) were obtained from the National Cancer Institute (NCI) Mouse Models of Human Cancers Consortium, brought to a full C57BL/6 background (Scarlett et al., 2012), and bred to TLR5-deficient (*Tlr5*$^{-/-}$) mice (B6.129S1-*Tlr5*^{tm1Flv}/J) (Cubillos-Ruiz et al., 2009). Galectin-1-deficient (*Lgals1*$^{-/-}$) mice were provided by G.A. Rabinovich at the Instituto de Biología y Medicina Experimental (IBYME-CONICET) Argentina and were originally generated by F. Poirier (Jacques Monod Institut). γδ T cell-deficient mice *Tcrd*$^{-/-}$ mice (B6.129P2-*Tcrd*^{tm1Mom}/J) were obtained from The Jackson Laboratory and bred to *Tlr5*$^{-/-}$ mice. WT C57BL/6 mice were obtained from the NCI. OT1 C57BL/6-Tg (TcraTcrb)1100Mjb/J and IL-6-deficient (B6.129S2-*IL6*^{tm1kopf}/J) transgenic mice were obtained from The Jackson Laboratory. All animals were maintained in pathogen-free barrier facilities. All experiments were conducted according to the approval of the Institutional Animal Care and Use Committee of the Wistar Institute.

Genetic Tumor Models and Cell Lines

Autochthonous p53/Kras flank sarcomas were initiated by subcutaneous delivery of 2.5×10^8 plaque-forming units of adenovirus-cre (Gene Transfer Vector Core, University of Iowa) into transgenic mice. For the mixed bone marrow chimeras, transgenic mice were irradiated for two consecutive days with 650 rads, followed by reconstitution with WT or *Lgals1*$^{-/-}$ bone marrow mixed at a 1:1 ratio with *Tcrd*$^{-/-}$ bone marrow. Flank tumors were initiated in reconstituted animals 6 weeks following engraftment. ID8 cells were provided by K. Roby (Department of Anatomy and Cell Biology, University of Kansas) and retrovirally transduced to express *Defb29* and *Vegf-a* (Conejo-Garcia et al., 2004). MPKAS cells were generated from passaging sorted tumor cells (CD45-negative) derived from mechanically disassociated autochthonous p53/Kras axillary sarcomas. Mouse ovarian tumor UPK10 cells were generated by culturing a mechanically dissociated p53/Kras primary ovarian tumor mass (Scarlett et al., 2012). The A7C11 and BRPKP110 primary mammary tumor cell lines were generated by passaging sorted tumor cells from mechanically disassociated p53/Kras (A7C11) or p53/Kras/myristoylated p110α (BRPKP110) mammary carcinomas (Rutkowski et al., 2014). Flank tumors with MPKAS- or MPKAS shRNA-expressing clones (1×10^5 cells), UPK10, and ID8-*Vegf-Defb29* (10^6) were admixed at a 1:1 ratio with growth factor-reduced Matrigel (BD Biosciences) and injected into the axillary flank. A7C11 tumors were initiated by injecting 2×10^4 cells into the axillary flank. Intraperitoneal ID8-*Vegf-Defb29* tumors were initiated by intraperitoneal injection of 2×10^6 cells. The tumor volume was calculated as: $0.5 \times (L \times W^2)$, where L is length, and W is width.

Human Specimens

Human ovarian carcinoma tissues were procured under a protocol approved by the Committee for the Protection of Human Subjects at Dartmouth-Hitchcock Medical Center (#17702) and under a protocol approved by the Institutional Review Board at Christiana Care Health System (#32214) and the Institutional Review Board of The Wistar Institute (#21212263). Human breast tumor tissues and sera were obtained under a protocol approved by the Institutional Review Board of the University of Pennsylvania (#805139) and the Institutional Review Board of The Wistar Institute (#21204259). Informed consent was obtained from all subjects.

ACCESSION NUMBERS

Deep sequencing analysis of the microbiota is available in the Sequence Read Archive (SRA) database (http://www.ncbi.nlm.nih.gov/sra) under the accession number SRP045910.

SUPPLEMENTAL INFORMATION

Supplemental Information includes Supplemental Experimental Procedures and seven figures and can be found with this article online at http://dx.doi.org/10.1016/j.ccell.2014.11.009.

AUTHOR CONTRIBUTIONS

M.R.R. designed, performed, and analyzed most experiments and cowrote the manuscript. T.L.S. provided intellectual and technical support and characterized clinical specimens. N.S. performed immunohistochemistry and contributed to the design of in vitro experiments. M.J.A., A.P.P., E.B., and A.J.T. contributed to the design of in vivo experiments and performed in vitro experiments. X.E.F. performed the identification of R392X carriers. J.N. processed and stored clinical specimens. M.G.C. and J.T. provided clinical specimens and expertise. R.Z. provided intellectual support and helped to interpret experimental results. G.A.R. and M.S. provided expertise in the biology of galectin-1 and the KO model and helped with writing the manuscript and interpreting experiments. J.R.C.G. oversaw and designed the study and experiments, analyzed data, and cowrote the manuscript.

ACKNOWLEDGMENTS

Support for shared resources was provided by Cancer Center Support Grant CA010815 (to The Wistar Institute). We thank P. Wickramasinghe for outstanding bioinformatical analysis, C. Huangci for technical support, and Dr. F. Bushman and A. Bailey (UPenn Viral/Molecular Core) for the analysis of microbiota. This study was supported by Grants R01CA157664, R01CA124515, R01CA178687, U54CA151662, and P30CA10815 and by Breast Cancer Alliance and Ovarian Cancer Research Fund Program Project Development awards. M.J.A. and N.S. were supported by Grant T32CA009171. A.P.P. was supported by the Fundación Alfonso Martín Escudero. A.J.T. was a nested Teal Scholar in Department of Defense Grant OC100059.

Received: April 25, 2014
Revised: August 29, 2014
Accepted: November 8, 2014
Published: December 18, 2014

REFERENCES

Abt, M.C., Osborne, L.C., Monticelli, L.A., Doering, T.A., Alenghat, T., Sonnenberg, G.F., Paley, M.A., Antenus, M., Williams, K.L., Erikson, J., et al. (2012). Commensal bacteria calibrate the activation threshold of innate antiviral immunity. Immunity *37*, 158–170.

Casanova, J.L., Abel, L., and Quintana-Murci, L. (2011). Human TLRs and IL-1Rs in host defense: natural insights from evolutionary, epidemiological, and clinical genetics. Annu. Rev. Immunol. *29*, 447–491.

Clarke, T.B., Davis, K.M., Lysenko, E.S., Zhou, A.Y., Yu, Y., and Weiser, J.N. (2010). Recognition of peptidoglycan from the microbiota by Nod1 enhances systemic innate immunity. Nat. Med. *16*, 228–231.

Conejo-Garcia, J.R., Benencia, F., Courreges, M.C., Kang, E., Mohamed-Hadley, A., Buckanovich, R.J., Holtz, D.O., Jenkins, A., Na, H., Zhang, L., et al. (2004). Tumor-infiltrating dendritic cell precursors recruited by a beta-defensin contribute to vasculogenesis under the influence of Vegf-A. Nat. Med. *10*, 950–958.

Cubillos-Ruiz, J.R., Engle, X., Scarlett, U.K., Martinez, D., Barber, A., Elgueta, R., Wang, L., Nesbeth, Y., Durant, Y., Gewirtz, A.T., et al. (2009). Polyethylenimine-based siRNA nanocomplexes reprogram tumor-associated dendritic cells via TLR5 to elicit therapeutic antitumor immunity. J. Clin. Invest. *119*, 2231–2244.

Dalotto-Moreno, T., Croci, D.O., Cerliani, J.P., Martinez-Allo, V.C., Dergan-Dylon, S., Méndez-Huergo, S.P., Stupirski, J.C., Mazal, D., Osinaga, E., Toscano, M.A., et al. (2013). Targeting galectin-1 overcomes breast cancer-associated immunosuppression and prevents metastatic disease. Cancer Res. *73*, 1107–1117.

Gewirtz, A.T., Vijay-Kumar, M., Brant, S.R., Duerr, R.H., Nicolae, D.L., and Cho, J.H. (2006). Dominant-negative TLR5 polymorphism reduces adaptive immune response to flagellin and negatively associates with Crohn's disease. Am. J. Physiol. Gastrointest. Liver Physiol. *290*, G1157–G1163.

Hawn, T.R., Verbon, A., Lettinga, K.D., Zhao, L.P., Li, S.S., Laws, R.J., Skerrett, S.J., Beutler, B., Schroeder, L., Nachman, A., et al. (2003). A common dominant TLR5 stop codon polymorphism abolishes flagellin signaling and is associated with susceptibility to legionnaires' disease. J. Exp. Med. *198*, 1563–1572.

Hawn, T.R., Scholes, D., Li, S.S., Wang, H., Yang, Y., Roberts, P.L., Stapleton, A.E., Janer, M., Aderem, A., Stamm, W.E., et al. (2009). Toll-like receptor polymorphisms and susceptibility to urinary tract infections in adult women. PLoS ONE *4*, e5990.

Hugot, J.P., Zaccaria, I., Cavanaugh, J., Yang, H., Vermeire, S., Lappalainen, M., Schreiber, S., Annese, V., Jewell, D.P., Fowler, E.V., et al.; IBD International Genetics Consortium (2007). Prevalence of CARD15/NOD2 mutations in Caucasian healthy people. Am. J. Gastroenterol. *102*, 1259–1267.

Iida, N., Dzutsev, A., Stewart, C.A., Smith, L., Bouladoux, N., Weingarten, R.A., Molina, D.A., Salcedo, R., Back, T., Cramer, S., et al. (2013). Commensal bacteria control cancer response to therapy by modulating the tumor microenvironment. Science *342*, 967–970.

Jackson, E.L., Willis, N., Mercer, K., Bronson, R.T., Crowley, D., Montoya, R., Jacks, T., and Tuveson, D.A. (2001). Analysis of lung tumor initiation and progression using conditional expression of oncogenic K-ras. Genes Dev. *15*, 3243–3248.

Jonkers, J., Meuwissen, R., van der Gulden, H., Peterse, H., van der Valk, M., and Berns, A. (2001). Synergistic tumor suppressor activity of BRCA2 and p53 in a conditional mouse model for breast cancer. Nat. Genet. *29*, 418–425.

Kryczek, I., Banerjee, M., Cheng, P., Vatan, L., Szeliga, W., Wei, S., Huang, E., Finlayson, E., Simeone, D., Welling, T.H., et al. (2009). Phenotype, distribution, generation, and functional and clinical relevance of Th17 cells in the human tumor environments. Blood *114*, 1141–1149.

Mazmanian, S.K., Round, J.L., and Kasper, D.L. (2008). A microbial symbiosis factor prevents intestinal inflammatory disease. Nature *453*, 620–625.

Misch, E., and Hawn, T. (2008). Toll-like receptor polymorphisms and susceptibility to human disease. Clinical science (London, England: 1979) *114*, 347–360.

Peng, G., Wang, H.Y., Peng, W., Kiniwa, Y., Seo, K.H., and Wang, R.F. (2007). Tumor-infiltrating gammadelta T cells suppress T and dendritic cell function via mechanisms controlled by a unique toll-like receptor signaling pathway. Immunity *27*, 334–348.

Rabinovich, G.A., and Croci, D.O. (2012). Regulatory circuits mediated by lectin-glycan interactions in autoimmunity and cancer. Immunity *36*, 322–335.

Rubinstein, N., Alvarez, M., Zwirner, N.W., Toscano, M.A., Ilarregui, J.M., Bravo, A., Mordoh, J., Fainboim, L., Podhajcer, O.L., and Rabinovich, G.A. (2004). Targeted inhibition of galectin-1 gene expression in tumor cells results in heightened T cell-mediated rejection; A potential mechanism of tumor-immune privilege. Cancer Cell *5*, 241–251.

Rutkowski, M.R., Allegrezza, M.J., Svoronos, N., Tesone, A.J., Stephen, T.L., Perales-Puchalt, A., Nguyen, J., Zhang, P.J., Fiering, S.N., Tchou, J., and Conejo-Garcia, J.R. (2014). Initiation of metastatic breast carcinoma by targeting of the ductal epithelium with adenovirus-cre: a novel transgenic mouse model of breast cancer. J. Vis. Exp. *26*.

Ryzhov, S., Novitskiy, S.V., Goldstein, A.E., Biktasova, A., Blackburn, M.R., Biaggioni, I., Dikov, M.M., and Feoktistov, I. (2011). Adenosinergic regulation of the expansion and immunosuppressive activity of CD11b+Gr1+ cells. J. Immunol. *187*, 6120–6129.

Sampath, V., Garland, J.S., Le, M., Patel, A.L., Konduri, G.G., Cohen, J.D., Simpson, P.M., and Hines, R.N. (2012). A TLR5 (g.1174C > T) variant that encodes a stop codon (R392X) is associated with bronchopulmonary dysplasia. Pediatr. Pulmonol. *47*, 460–468.

Scarlett, U.K., Rutkowski, M.R., Rauwerdink, A.M., Fields, J., Escovar-Fadul, X., Baird, J., Cubillos-Ruiz, J.R., Jacobs, A.C., Gonzalez, J.L., Weaver, J., et al.

(2012). Ovarian cancer progression is controlled by phenotypic changes in dendritic cells. J. Exp. Med. *209*, 495–506.

Toscano, M.A., Bianco, G.A., Ilarregui, J.M., Croci, D.O., Correale, J., Hernandez, J.D., Zwirner, N.W., Poirier, F., Riley, E.M., Baum, L.G., and Rabinovich, G.A. (2007). Differential glycosylation of TH1, TH2 and TH-17 effector cells selectively regulates susceptibility to cell death. Nat. Immunol. *8*, 825–834.

Viaud, S., Saccheri, F., Mignot, G., Yamazaki, T., Daillère, R., Hannani, D., Enot, D.P., Pfirschke, C., Engblom, C., Pittet, M.L., et al. (2013). The intestinal microbiota modulates the anticancer immune effects of cyclophosphamide. Science *342*, 971–976.

Wang, L., Yi, T., Kortylewski, M., Pardoll, D.M., Zeng, D., and Yu, H. (2009). IL-17 can promote tumor growth through an IL-6-Stat3 signaling pathway. J. Exp. Med. *206*, 1457–1464.